

Energy Evolution in Deep-Buried Roadway upon Excavation

Ziyun Li^{1,2,*}, Guang Wu¹, Guoqiang Liu³, Xiaoping Wang² and C.R. Thomson⁴

¹Faculty of Geosciences and Environmental Engineering, Southwest Jiaotong University, Chengdu, Sichuan 611756, China

²School of Civil Engineering and Architecture, Chongqing University of Science and Technology, Chongqing 401331, China

³China Railway 19th Bureau Group Sixth Engineering Co., Ltd., Wuxi, Jiangsu 214028, China

⁴Department of Geography and Earth Sciences, Aberystwyth University, Ceredigion, SY23 3DB, United Kingdom

Received 9 May 2018; Accepted 13 September 2018

Abstract

Energy evolution is a key factor to catastrophe during an excavation of deep rock mass. Existing energy analysis methods are only limited to changes in elastic strain energies before and after the excavation. These methods neglect energy concentration and energy dissipation characteristics of rock units during the excavation. This study aims to investigate energy evolution and redistribution laws in surrounding rock mass caused by excavation of deep-buried roadway. Thus, a numerical calculation of total strain energy, elastic strain energy, dissipated energy, energy concentration efficiency, and energy dissipation efficiency of surrounding rock mass was conducted in a deep-buried roadway of Linglong Gold Mine in Shandong Province, China. Energy concentration, accumulation and dissipation characteristics, and energy accumulation and dissipation efficiency of rock units upon excavation in the deep-buried roadway were explored through a contrastive analysis of the distribution of these energy indexes. Results demonstrate that the influence depth of radial excavation disturbance of this roadway is 5 times the roadway diameter (15 m), and the axial influence depth is approximately 3 times the roadway diameter (10 m). The energy dissipation efficiencies from the sidewall to the corner of the roadway are relatively high at 96% and 57%. The roof and floor of the roadway are stable given the relatively high energy accumulation efficiency, 95% and 67% respectively. The location of rockburst in the engineering field observation conforms to the high energy dissipation of rock units in the numerical calculation. Therefore, the constructed energy analysis method is effective and promising. The conclusions provide reasonable guidance to the stability of deep-buried roadways and rockburst predictions.

Keywords: Deep-buried roadway, Energy evolution, Numerical analysis, Secondary development

1. Introduction

Stability analysis and optimization design of a deep-buried roadway excavation under high geo-stress are difficulties encountered in underground engineering worldwide. Influenced by crustal motion, high geo-stress field, and exogenic geological process, the stability and safety problems in the deep-buried roadway are important and demand strict requirements on construction and excavation. The inoculation and occurrence of underground engineering geological disaster under high geo-stress are a nonlinear evolution process. Different excavation order, method, and control measures will generate various mechanical effects. Thus, studying surrounding rock stability and disaster evaluation indexes in a deep-buried roadway and guiding the optimization of a construction program provide important research values to guarantee engineering safety and stability.

The bearing capacity of rocks is related to stress state. Evaluation indexes generally refer to compression resistance, tensile strength, and shear strength of rocks. In terms of energy, the rock abilities of energy absorption, dissipation, and release are methods for evaluating the bearing capacity of rocks. The law of thermodynamics states that energy transformation is a substantive characteristic of the physical

process of substances. The rupture of the rock is the final result of an energy-driven destabilization process [1]. Therefore, studying energy change law during stress-induced damages and failures of rock masses and describing rock deformation and failure law through energy analysis method can provide a new perspective and solution to rock engineering practice.

Rock failure is the process of accumulating, dissipating, and releasing strain energies in rocks. During rock deformation and failure, internal energy conversion conforms to the first law of thermodynamics. In particular, different forms of energy remain constant in the transmission and conversion, that is, constant of total energy. In the loading process of a rock unit, energy has different forms, such as elastic energy, plastic, damage, kinetic, radiation, thermal energy and so on. Given that the excavation surface of a deep-buried roadway moves forward, the stored energy in rock units at different positions change continuously. Researchers who investigate the energy evolution of rock mass focus on energy release characteristics and rockburst disasters. These researchers predict rockburst or analyze rockburst tendency by the difference in elastic strain energy before and after an excavation but neglect energy dissipation characteristics [2]. In fact, energy evolution characteristics in a deep-buried roadway caused by excavation cover energy concentration, accumulation, dissipation, and release [3]. Geological disasters, such as rockburst, peeling, and large deformation,

*E-mail address: liziyun130@126.com

ISSN: 1791-2377 © 2018 Eastern Macedonia and Thrace Institute of Technology. All rights reserved.

doi:10.25103/jestr.114.21

are collaborative consequences of multiple energy characteristics.

Therefore, the evolution characteristic and distribution laws of multiple energy parameters of surrounding rocks after the deep-buried roadway excavation were analyzed by energy analysis theory and numerical analysis. This study aims to lay foundations for further research on the relationship between energy evolution and geological disasters (e.g., rockburst, peeling, and large deformation).

2. State of the art

On the basis of triaxial cyclic loading and unloading tests under different confining pressures and energy principle, Li et al. [4] studied the energy evolution laws during a loading process and established the rock strength failure criteria in accordance with the sudden changes in energy release and loss function. Sun et al. [5] combined energy with total and elastic deformation ratio and analyzed tunnel stability by energy changes in the original rocks, finally, they found that an energy overflow of the original rocks in a tunnel is the fundamental cause of tunnel instability after the excavation. To discuss rockburst in certain argillaceous sandstone and coal measure strata in surrounding rocks of deep-buried roadway, He et al. [6-11] designed different types of rockburst experimental methods by adopting an independently developed mechanics experimental system for deep well rockburst; then, these researchers reproduced the complicated mechanical phenomenon of the whole rockburst process in a laboratory. On the basis of experimental studies, these researchers disclosed the rockburst dynamic development process and crack propagation and energy variation laws. Important conclusions are as follows: the rockburst strength in coal mines is determined by the content of clay mineral components, and the rockburst pattern is influenced by bedding occurrences. These experimental studies have enriched energy evolution law and conversion characteristics in the loading process of rocks and have provided a theoretical basis for energy analysis during an excavation of underground rocks.

Currently, studies on energy evolution of surrounding rocks in deep underground engineering focus on energy release characteristics of rocks. For example, Xu et al. [2] proposed the rock burst energy release rate on the basis of the local energy release and energy ultimate storage ratios; these researchers aimed to simulate the surrounding rock damage and failure evolution process during the advancement of working face and analyze positions and strengths of rockburst in potentially dangerous regions. Their research results had certain reference values for designing rockburst prevention measures in deep constructions. Weng et al. [12] numerically studied strain energy density, an energy index in the rockburst process. These authors simulated energy accumulation and dissipation characteristics during the failure process and determined a direct relationship between large-scale energy release and rockburst. Jiang et al. [13] suggested a new energy index, namely, local energy release rate (LERR). These authors interpreted rockburst from the perspective of energy release by tracing the peak and valley amount of elastic strain energy before and after a brittle failure of rocks, thereby finding that energy release is the internal cause of rockburst. Moreover, these researchers predicted rockburst strength and depth using the LERR. On the basis of the basic theory of local energy release rate, Qiu et al. [14] proposed a

new evaluation numerical index of rockburst tendency, that is, relative energy release index. These researchers used this index to identify regions and positions with high strain-type rockburst risks and the scope of rock damage caused by excavating deep tunnel rocks. They provided a new theory and analysis tool for evaluating and preventing rockburst disasters and brittle failures in a deep tunnel. Su et al. [15] reflected elastic strain energy of rock unit storage using an elastic strain energy parameter and delineated the position and scope of surrounding rock burst by the difference of elastic strain energies before and after the excavation. A quantitative analysis of rockburst strength and its evolution characteristics in the excavation process was conducted. In the abovementioned studies, energy evolution characteristics of a rock unit are concentrated in elastic strain energy. Elastic strain energy is calculated using the stress and strain of rock units. It can reflect an energy storage state of a rock unit before and after an excavation of underground opening. In fact, the excavation process of underground opening is a stress redistribution process. Different degrees of energy concentration, accumulation, or release characteristics occur at various positions of a rock mass. These energy evolution characteristics must not be overlooked. Thus, analyzing energy evolution laws in deep-buried roadway, predicting rockburst, and evaluating rockburst tendency by a single energy parameter, that is, elastic strain energy, are unreasonable.

When the recorded microseism data were used to analyze energy release and predict rockburst, the recorded data can only reflect energy release characteristics. Mansurov [16] predicted a strong rockburst in mine engineering by using the microseism data from the energy release perspective. Zhuang et al. [17] revealed the energy-release patterns in the surrounding rock masses and their relationship with stability, thus providing a reference for identifying, delineating, and predicting potential danger areas in the surrounding rock masses for underground water-sealed oil storage caverns. Wang et al. [18] described stress concentration and energy release of rock masses using the earthquake speed chromatography and rockburst energy recorded diagram. The results were verified by two actual cases of Xing'an Coal Mine, Hegang, China. In the abovementioned studies, a microseism of field monitoring records and rockburst energy data reflects actual energy release characteristics. Although energy release is a characteristic of rockburst occurrence, rock units with different energy dissipation characteristics may result in various rockburst intensities. Therefore, analyzing rockburst disasters by combining energy release and dissipation characteristics is reasonable.

The stored energy in rock units changes continuously with the advancement of the working face of deep tunnels. In this process, strain energy is released at several positions but accumulated in other positions, thereby resulting in different mechanical responses of an underground tunnel under a dynamic disturbance. Wang et al. [19] conducted a numerical study of rockburst in a deep-buried roadway and found that an unloading effect causes rock fracture and rapid release of strain energy. However, rock fracture occurred on a wedge. During rockburst development, microcracks in the surrounding rocks of the tunnel were located and crossed and finally evolved into a group of concentrated "V"-shaped damage belt. Under general situations, rock failure behaviors, such as rockburst and peeling, in deep underground engineering occurred suddenly under the brittle state without prior evident symbol [20-24]. Li et al. [25] examined the

dynamic response and strain energy evolution in a deep-buried roadway with a straight-wall-top-arch section by using an implicit–explicit sequence solution and discovered the relationships between lateral stress coefficient and compressive fracture behavior and strain energy release of holes. Li et al. [26] constructed a theoretical formula for evaluating a dynamic stress concentration factor that surrounds the round hole under explosive stress wave incidence conditions and analyzed dynamic responses that surround the tunnel from perspectives of dynamic stress concentration and energy evolution. These researchers found that the reduction of strain energy and residual kinetic energy are positively correlated with the lateral stress coefficient and buried depth of tunnel; moreover, under the same conditions, residual kinetic energy was significantly higher than reduction of strain energy. In the abovementioned studies, energy release behavior was analyzed from the perspective of dynamic disturbance. However, studies have only analyzed a dynamic response to explosive excavation from the perspective of energy release and have not qualitatively reflected energy accumulation and dissipation under dynamic disturbance of deep-buried roadway.

To address existing research shortcomings, several energy parameter indexes that can reflect energy accumulation, release, and dissipation characteristics were proposed and simulated in numerical analysis software FLAC^{3D}, which is convenient for analyzing distributions of energy parameters in surrounding rocks after the deep-buried roadway excavation. On the basis of the 500 m deep-buried roadway in Linglong Gold Mine in Shandong Province, China, energy distribution characteristics and evolution laws (including energy concentration, accumulation, and dissipation) of rock mass during the excavation were analyzed by energy theory and numerical simulation analysis. The research results enrich the energy evolution mechanism study and provide a new perspective for energy evolution laws in surrounding rocks of deep-buried roadway. The research conclusions have an important engineering significance to excavation stability evaluation and rockburst prediction in deep-buried roadway.

The remainder of this study is organized as follows. Section 3 introduces the energy calculation method and numerical model for surrounding rocks in deep-buried roadway. Section 4 exhibits energy evolution and distribution features in the deep-buried roadway of Linglong Gold Mine and analyzes the corresponding results. Section 5 presents conclusions drawn from this study.

3. Methodology

3.1 Energy Analysis Principle

Several important hypotheses were presented to deduce the expressions of energy parameters. First, a rock unit makes no heat exchange with the external environment in a closed system. Second, lithology is continuous, uniform, and isotropous. Moreover, the initial geo-stress in the roadway excavation scope distributes uniformly, and excavation will be influenced by far-field geo-stress continuously. During the load-bearing process of the rock mass unit, a part of the input energy from the external environment is accumulated in the rock unit as the elastic strain energy U^e . This part of the input energy is reversible and released after unloading. The rest energy is dissipated energy U^d and consumed by

plastic deformation, crack growth, and kinetic energy release. This part of the energy is irreversible.

The typical compressive stress–strain curve of a rock unit is illustrated in Fig. 1. The area U_i^d refers to the energy consumed by rock damage and plastic deformation. Changes in U_i^d conform to the second law of thermodynamics. In particular, the internal state changes conform to the increase in entropy. The shadow region U_i^e reflects accumulated elastic strain energy in rocks that can be released. The sum of U_i^d and U_i^e is the total strain energy U . From the thermodynamics perspective, energy dissipation is one-way and irreversible, whereas energy accumulation and release are two-way under certain conditions.

Each part of the rock element energy in the principal stress space can be calculated as [1]:

$$U = U^e + U^d \quad (1)$$

$$U = \int_0^{\varepsilon_1} \sigma_1 d\varepsilon_1 + \int_0^{\varepsilon_2} \sigma_2 d\varepsilon_2 + \int_0^{\varepsilon_3} \sigma_3 d\varepsilon_3 \quad (2)$$

$$U^e = \frac{1}{2} \sigma_1 \varepsilon_1^e + \frac{1}{2} \sigma_2 \varepsilon_2^e + \frac{1}{2} \sigma_3 \varepsilon_3^e \quad (3)$$

$$\varepsilon_i^e = \frac{1}{E_i} [\sigma_i - \nu_i (\sigma_j + \sigma_k)] \quad (4)$$

where U is the total strain energy; U^e is elastic strain energy; $\sigma_1, \sigma_2,$ and σ_3 are the first, second, and third principal stresses, correspondingly; $\varepsilon_1, \varepsilon_2,$ and ε_3 are the first, second, and third principal strains; $\varepsilon_1^e, \varepsilon_2^e,$ and ε_3^e are elastic strains in the three directions of principal stress, respectively; E_i is the unloading elastic modulus; and ν_i is the unloading Poisson's ratio.

Energy conversion from rock deformation to buckling failure is a dynamic process that is manifested by conversion and balance among full strain energy, releasable elastic strain energy, and dissipated energy. Several specific energy states correspond to any moment in the rock deformation process. These energy states are the function of stress, strain, and time and related to current stress, strain state, and historical stress path of the rock unit.

Equation 2 is simplified by using the Einstein summation convention. Thus,

$$U = \sum_{j=1}^n (\sigma_1^j \bullet \Delta \varepsilon_1^j + \sigma_2^j \bullet \Delta \varepsilon_2^j + \sigma_3^j \bullet \Delta \varepsilon_3^j) \quad (5)$$

where n is the number of calculation sections of the stress–strain curve at any moment t , j is the section point, and the stress σ and strain ε with a superscript of j represent the stress and strain at point j , correspondingly.

Equation (5) is the sum of products of stress and strain increments. This equation is applicable to calculating the total strain energy of rock units under different types of constitutive model. In addition, it can be used to calculate the total strain energy under different stress histories and paths. This energy index (positive at compression and negative at tension) is the sum function of stress and strain increments and can reflect concentrated energy in the rock unit under the external forces (including geo-stress and artificial excavation disturbance).

In Equations (3) and (4), the elastic strain energy accumulated in the rock unit is related to the unloading elastic modulus E_i and unloading Poisson's ratio $\bar{\nu}$ after the damage. Considering the orthotropic of rock units, the compressive stress positive is set. Therefore, Equation (3) can be rewritten as

$$\frac{1}{2}\sigma_i \epsilon_i^e = \frac{1}{2} \left[\frac{\sigma_1^2}{E_1} + \frac{\sigma_2^2}{E_2} + \frac{\sigma_3^2}{E_3} - \bar{\nu} \left[\left(\frac{1}{E_1} + \frac{1}{E_2} \right) \sigma_1 \sigma_2 + \left(\frac{1}{E_2} + \frac{1}{E_3} \right) \sigma_2 \sigma_3 + \left(\frac{1}{E_1} + \frac{1}{E_3} \right) \sigma_1 \sigma_3 \right] \right] \quad (6)$$

For convenient engineering applications, Equation (6) is simplified appropriately. Considering the average effect along the principal stress direction, the elastic strain energy can be rewritten as

$$U^e = \frac{1}{2E} \left[\sigma_1^2 + \sigma_2^2 + \sigma_3^2 - 2\bar{\nu}(\sigma_1\sigma_2 + \sigma_2\sigma_3 + \sigma_1\sigma_3) \right] \quad (7)$$

where \bar{E} is the unloading elastic modulus, and $\bar{\nu}$ is the unloading Poisson's ratio.

In Equation (7), elastic strain energy is the state function of principal stress and an elastic potential function. A high numerical value of the function indicates a highly accumulated releasable strain energy and large stress state. The stress state changes in the rock unit can be speculated from the evolution curve of the elastic strain energy.

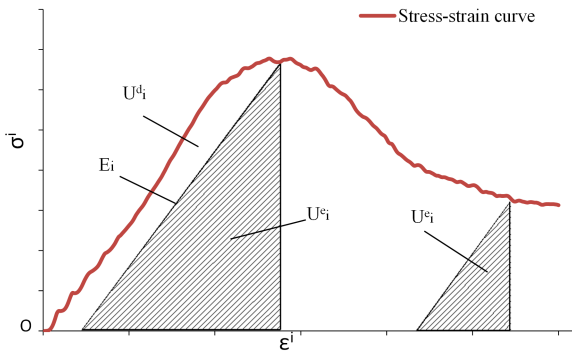


Fig. 1. Quantity relationship between elastic strain energy and dissipated energy in a rock unit

In accordance with the abovementioned energy theory, the typical stress-strain and energy evolution curve of rocks under compression conditions are calculated (Fig. 2). Clearly, in the elastic deformation stage of rocks (OA section), the total and elastic strain energy curves overlap, and the energy loss is nearly zero, thereby indicating that the total strain energy is converted into elastic strain energy completely and accumulates in rocks. In the plastic deformation stage (AB section), the internal microcrack in rocks propagates gradually into macroscopic cracks, and the plastic deformation occurs and intensifies gradually. At this moment, the total strain energy is converted into elastic strain energy and dissipated energy. The dissipated energy increases gradually from zero, whereas the accumulation efficiency of elastic strain energy reduces and reaches the maximum at the stress peak. In the stress drop section after the stress peak (CD section), that is, the overall rock fracture and cut-through process, energy dissipation increases quickly, and the growth rate approaches that of the total strain energy gradually. The elastic strain energy falls from the peak to the valley progressively, thereby indicating that fractured rocks have lost the ability of energy accumulation,

and most total strain energies have been converted into dissipated energy.

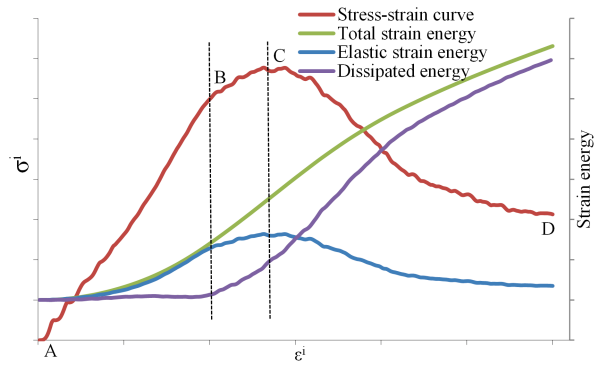


Fig. 2. Typical stress-strain and energy evolution curves of rock under pressure

3.2 Rock mass model and simulation setup

Linglong gold mine, located in Shandong province, is the largest and one of the most productive gold mines in China. It has been experiencing frequent unconventional rock failures (e.g. rockburst and spalling) in recent years. Owing to the geological and geo-environmental conditions, a shrinkage stopping method has been used in the mine for over 50 years since 1962. Recently, with the increase in mining depth, the stability of the mined-out areas has become a significant problem. Since the existence of unfilled mined-out areas round excavations, rockburst has become an ongoing problem that should be investigated (Fig. 3) [12].



Fig. 3. (a) Spalling in transport roadway; (b) Rockburst in destress roadway[12]

In this study, the roadway that is approximately 500 m deep in the Linglong Gold Mine is used as the research object. The maximum principal stress at 500 m depth reaches 29.9 MPa and is perpendicular to the axial direction of the roadway. The horizontal principal stress is 13.9 MPa and is parallel with the axial direction of the roadway. The vertical principal stress is 15.3 MPa. The roadway is far from the major vein and is unaffected by other gobs or cavities. Furthermore, the gold ore vein is very thin and long (like a flat rope), compared with the granite surroundings. [12]. Thus, using the homogeneous rock material to model the underground opening is justified. The corresponding parameters are listed in Table 1. During the excavation process, the region from the lower sidewall of the advancing working surface to the floor of the roadway developed fierce rockbursts.

Table 1. Properties of rock mass

Young's modulus (GPa)	Tensile strength (MPa)	Poisson's ratio	Friction angle (°)	Cohesion (MPa)
30.46	5.36	0.24	51	55.1

The cross-section type of the roadway is shaped as a straight-wall-top-arch with a size of 3.0 × 3.5 m. Only half of the numerical model is established considering the symmetry of the roadway. To eliminate the boundary effect of the model, the horizontal size (x), vertical size (z), and longitudinal size (y) of the model are set 10 times the diameter of 15 m, 10 times the diameter of 34 m, and 35 m in accordance with experiences, correspondingly. A geo-stress is applied to the model. The upper boundary is applied with a vertical stress to simulate the dead loads of the overlying rock strata. The surrounding boundaries and lower boundary use the displacement constraint boundaries, and the displacement is fixed. Considering the calculation speed and simulation accuracy, surrounding rock grids close to the roadway are encrypted appropriately (Fig. 4). The roadway contains single lithological surrounding rocks and applies a strain-softening constitutive model.

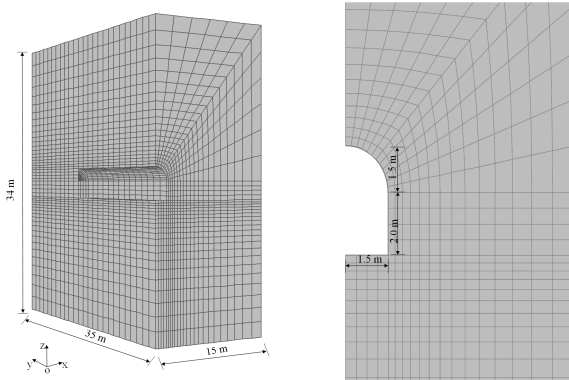


Fig. 4. Meshed model with dimensions

4. Result Analysis and Discussion

4.1 Strain energy evolution and distribution

The rock unit is considered in a triaxial compression state in the initial geo-stress and can accumulate abundant strain energies. Under this circumstance, rock units are generally in the elastic state, and the accumulated energy is elastic strain energy [5]. The accumulated energy in rock units under the effect of initial geo-stress is

$$U_0^e = \frac{1}{2E} [\sigma_1^2 + \sigma_2^2 + \sigma_3^2 - 2\nu(\sigma_1\sigma_2 + \sigma_2\sigma_3 + \sigma_1\sigma_3)] \quad (8)$$

where U_i^e is the initial elastic strain energy stored in rock units under geo-stress, and $\sigma_1, \sigma_2,$ and σ_3 are the first, second, and third principal stresses under the initial geo-stress, respectively.

The elastic strain energy distribution on surrounding rocks of the roadway at 20 m of advancing distance is depicted in Fig. 5. The energy accumulation behavior is the strongest at the roof of the roadway, followed by the floor. The maximum energy accumulation has reached 87.76 kJ. The elastic strain energy at the sidewall is lower than 10 kJ, which is lower than the average energy accumulation of the surrounding strata. This result reflects that the sidewall has energy release and dissipation behaviors.

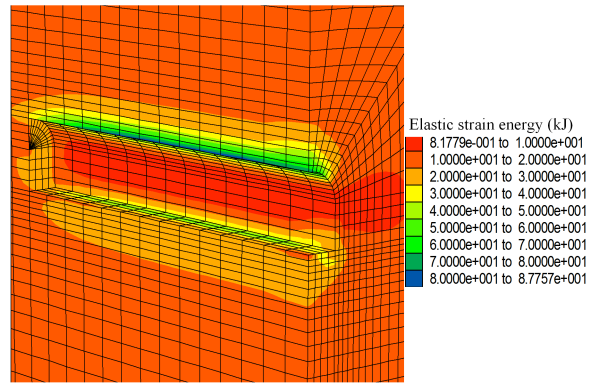


Fig. 5. Elastic strain energy distribution in the surrounding ground

To study the energy distribution in the surrounding rocks near and far from the excavation profile of the roadway, the energy parameters of rock units at five typical positions (i.e., roof, spandrel, sidewall, corner, and floor of the roadway) 0.5, 1, 1.5, 2, 2.5, and 5 times the diameter in the Y=10 m section are monitored (Fig. 6).

To examine the strain energy distribution of the excavation profile along the axial direction of the roadway, the energy parameter distribution curves at different sections with -20, -15, -10, -5, 0, 5, and 10 m distance away from the profile after a one-off excavation are demonstrated in Fig. 7.

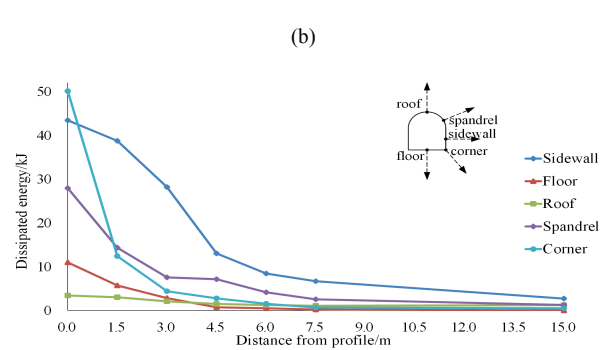
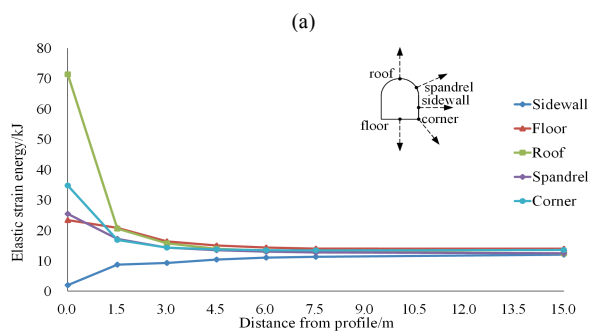
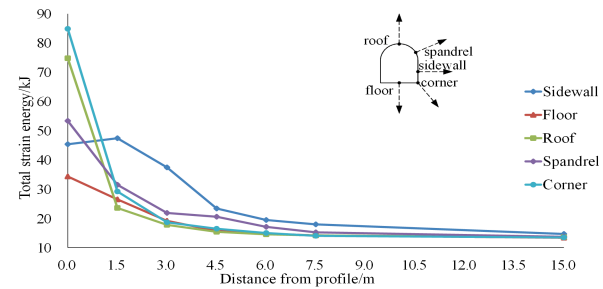


Fig. 6. Strain energy evolutions along five different directions from the excavation profile on the Y=10 m section. (a) Total strain energy. (b) Elastic strain energy. (c) Dissipated energy

Fig. 6 exhibits that the energy parameter distribution features at various excavation profiles are significantly different. Energy dissipation and release at the corner and sidewall of the roadway are the most violent and close to the rockburst position in the field observation. With the increase in distance to the profile surface, the energy parameters at all positions, except elastic strain energy at the sidewall, decreases gradually. When the distance is higher than 5 times the diameter, all energy parameter distribution becomes uniform. The total and elastic strain energies approach the initial strain energy, which is approximately 13 kJ, under the original geo-stress conditions gradually. Simultaneously, the dissipated energy becomes zero gradually. These results demonstrate that the radial influence depth of the excavation disturbance of this roadway is approximately 5 times the diameter of the roadway.

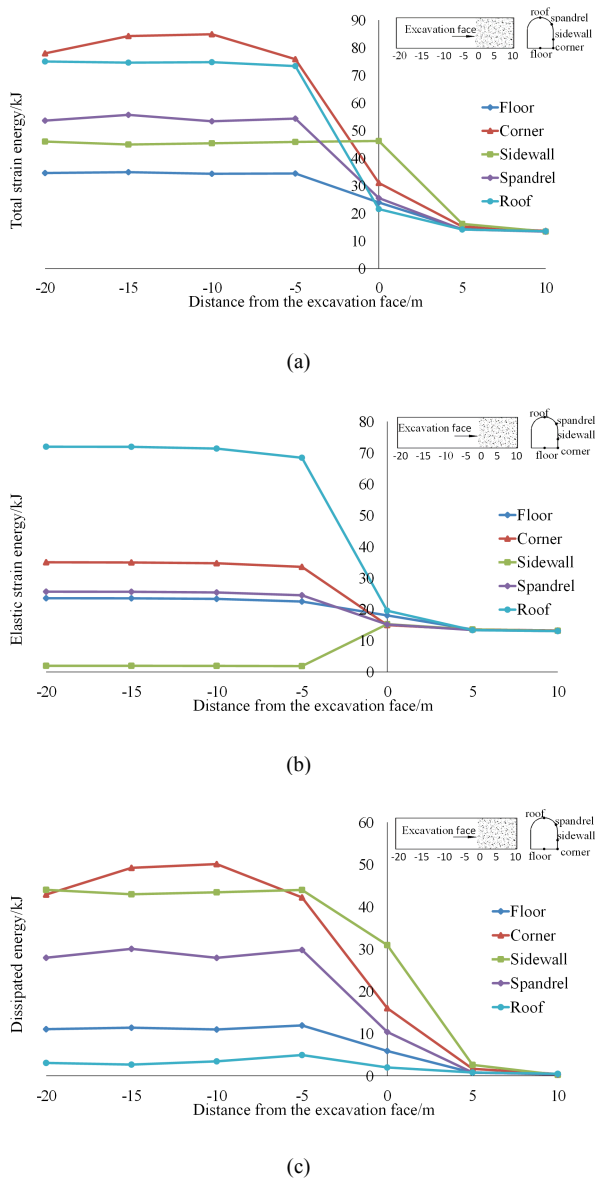


Fig. 7. Energy parameters for rock units at the roof, sidewall, floor, spandrel, and corner of the roadway along axial direction with the corresponding distance of -20, -15, -10, -5, 0, 5, and 10 m from profile. (a) Total strain energy. (b) Elastic strain energy. (c) Dissipated energy

In Fig. 7, the total and elastic strain energies at different positions in the non-excavated rock mass in 5–10 m front of the excavation surface approach the initial strain energy

(approximately 13 kJ) under the original geo-stress conditions. The energy dissipation becomes zero gradually. This result confirms that deep rock units that are further away from the excavation surface are minimally influenced by excavation disturbance, and the rock units beyond the 10 m front of the excavation surface are essentially undamaged and still in the initial geo-stress state. The axial influence depth of the excavation disturbance of the roadway is approximately 10 m. The distributions of energy parameters at different excavated roadway positions along the axial direction are consistent. Only the total strain energy and dissipated energy at the corner of the roadway are observed in the range from -15 m to -10 m are high. This range is near the field observed position of rockburst.

4.2 Energy accumulation efficiency (EAE) and energy dissipation efficiency (EDE) distribution analyses

In accordance with the energy analysis principle in Section 3, the mean of energy parameters in the excavation region from -20 m to 0 m is obtained. The relations of the total strain energy on the excavation surface with the EAE and EDE are displayed in Fig. 8. The calculation formulas of energy efficiency are

$$EAE = \frac{U^e}{U} \quad (9)$$

$$EDE = \frac{U^d}{U} \quad (10)$$

The sidewall dissipates larger amount of energies, and the EDE reaches 96%. Energy accumulation is dominant at the roof and floor of the roadway with EAEs of 95% and 67%, respectively. The energy accumulation and dissipation at the spandrel and corner of the roadway are equivalent.

The relationships of the total strain energy in different positions reflect that the maximum total strain energy is achieved at the corner and roof of the excavated roadway with close numerical values, as presented in Fig. 8. However, a large gap is observed between the energy accumulation and dissipation of the two positions. Energy accumulation is dominant at the roof of the roadway, and the EAE is 19 times the EDE. The energy accumulation and dissipation behaviors at the corner of the roadway are equivalent. Moreover, energy dissipation is slightly advantageous. However, the energy dissipation amount is 13 times that at the roof of the roadway. On the basis of the comprehensive analysis on stress distribution surrounding the roadway and profile shape, the geo-stress perpendicular to the axis of the roadway is redistributed after excavation, and energies are partly dissipated and released at the excavation face from the sidewall, which is perpendicular to the principal geo-stress at the corner of the roadway. These results conform to the field observation of fierce rockburst and spalling accidents that occurred 11 m away from the excavation surface. The remaining energies deflect with stress and transmit from the spandrel to the roof and from the corner to the floor of the roadway. The arc roadway spandrel is beneficial for energy transmission, thereby resulting in a high energy accumulation at the roof of the roadway. However, singular points, such as the corner of the roadway, are against stress transmission and energy accumulation; thus, energy dissipation and release are dominant at the corner of the

roadway. This result indirectly causes the EAE to be lower at the floor than at the roof of the roadway.

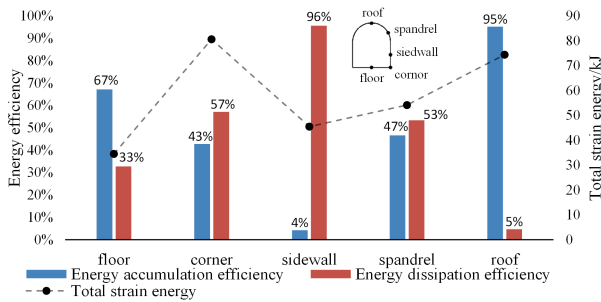


Fig. 8. Comparison of EAE and EDE at various parts of the excavated profile

On the basis of the abovementioned analyses, rock units with a high EAE have less energy dissipation and release. Thus, they do not develop failures or only have minimal damage. For rock units with a high EDE, abundant energies are dissipated or released. Energies are consumed by plastic deformation and crack propagation or released as kinetic energy. In hard rocks, rock units with a high EDE are easy-to-develop rockbursts or spalling failure parallel to the excavation surface in the high geo-stress environment.

The surrounding rock energy accumulation and dissipation can be predicted using the surrounding geo-stress distribution and profile excavation shape in the roadway. Moreover, the EAE and EDE at different positions along the excavation profile line can be speculated. The results of this study are conducive to formulating a feasible and effective support program and reducing occurrence risks of rockburst in the deep-buried roadway.

5. Conclusions

To study energy evolution laws and distribution after excavating deep-buried roadway, the physical significance and conversion relationships between total strain energy, elastic strain energy, and dissipated energy were analyzed using the energy analysis principle discussed in Section 3. A numerical simulation analysis on the evolution and distribution laws of the total strain energy, elastic strain energy, dissipated energy, EAE, and EDE upon excavation of the approximately 500 m deep roadway in Linglong Gold Mine in Shandong Province, China was conducted. The following major conclusions could be drawn:

The radial influence depth of the excavation disturbance of the deep-buried roadway in Linglong Gold Mine is 5 times the diameter of 15 m, and the axial influence depth is approximately 3 times the diameter of 10 m. Rock units

beyond the sphere of influence hardly demonstrate energy dissipation behaviors.

Energy concentration, accumulation, and dissipation characteristics in rock units are related to excavation shape, geo-stress distribution, excavation position, and stress concentration in an underground roadway. The most serious energy evolution occurs in the region from the sidewall to the corner of the roadway near the excavation profile line in the deep-buried roadway of the Linglong Gold Mine. The EDE is relatively higher at the two positions than at the other positions. The two positions conform to the field-observed occurrence positions of rockburst.

The maximum principal stress in the deep-buried roadway of the Linglong Gold Mine is the horizontal stress that is perpendicular to the axial direction of the roadway. The principal stress deflects upon excavation, thereby resulting in a higher EAE at the roof and floor of the roadway than at the other positions.

During roadway excavation in the hard rock and high geo-stress environment, the positions with high EDE and singular points, such as right-angle corners, are easy-to-develop rockbursts.

The proposed energy analysis method has an explicit concept, simple form, convenient calculation, and easy programming structure. The proposed method can also reflect energy concentration, accumulation, and dissipation characteristics well in deep-buried roadways and demonstrate EAE and EDE favorably in rock units at different positions. The results provide a new perspective for further studying the energy evolution law in surrounding rocks of deep-buried roadway. These results have important engineering significance to excavation stability evaluation and rockburst prediction in deep-buried roadway. However, dissipated energy in this study is simplified. Plastic deformation, crack propagation, and kinetic energy release are not further divided but considered comprehensively. Future studies must quantize kinetic energy parameters in dissipated energy, thereby laying foundations for further investigating the rockburst mechanism of deep-buried roadway.

Acknowledgements

The authors are grateful for the financial and general support provided for this research by the National Natural Science Foundation of China (Grant No. 41302223), the Chongqing Municipality and Housing Authority (Grant No. KJ-2015 047), and the Education Commission of Chongqing Municipality (Grant No. KJ1713327). The fund covers the costs to publish the work in open access.

This is an Open Access article distributed under the terms of the Creative Commons Attribution Licence



References

- Xie, H. P., Li, L. Y., Peng, R., Ju, Y., "Energy analysis and criteria for structural failure of rocks". *Journal of Rock Mechanics and Geotechnical Engineering*, 1(1), 2009, pp.11-20.
- Xu, J., Jiang, J., Xu, N., Liu, Q., Gao, Y., "A new energy index for evaluating the tendency of rockburst and its engineering application". *Engineering Geology*, 230, 2017, pp.46-54.
- Salamon, M. D. G., "Energy considerations in rock mechanics: fundamental results". *Journal- South African Institute of Mining and Metallurgy*, 84(8), 1984, pp.233-246.
- Li, Z. Y., Wu, G., Huang, T. Z., Liu, Y., "Variation of energy and criteria for strength failure of shale under triaxial cyclic loading". *Chinese Journal of Rock Mechanics & Engineering*, 37(03), 2018, pp. 662-670.

5. Sun, F., Feng, X. T., Zhang, C. Q., Zhou, H., Qiu, S. L., "Stability estimation method of greenschist tunnel based on increasing-decreasing energy method". *Rock & Soil Mechanics*, 33(2), 2012, pp.467-475.
6. He, M. C., Miao, J. L., Feng, J. L., "Rock burst process of limestone and its acoustic emission characteristics under true-triaxial unloading conditions". *International Journal of Rock Mechanics & Mining Sciences*, 47(2), 2010, pp.286-298.
7. He, M. C., Miao, J. L., Li, D. J., "Characteristics of acoustic emission on the experimental process of strain burst at depth". In: *The 7th international symposium on rockburst and seismicity in mines proceedings*, New York/New Jersey, USA: Rinton Press, 2009, pp.181-188.
8. Li, D. J., Jia, X. N., Feng, J. L., "Acoustic emissions and infrared characteristics of coal burst process". In: *The 7th international symposium on rockburst and seismicity in mines proceedings*. , New York/New Jersey, USA: Rinton Press, 2009, pp.1341-1346.
9. Miao, J. L., He, M. C., LI, D. J., "Stress wave characteristics in the process of strain coal burst experiments". In: *The 7th international symposium on rockburst and seismicity in mines proceedings*. , New York/New Jersey, USA: Rinton Press, 2009, pp.1347-1352.
10. He, M. C., Miao, J., Li, D., Wang, C., "Experimental study on rockburst processes of granite specimen at great depth". *Chinese Journal of Rock Mechanics & Engineering*, 26(5), 2007, pp.865-876.
11. Cai, M., Qiao, L., Li, C., Yu, B., Wang, S., "Results of in situ stress measurements and their application to mining design at five Chinese metal mines". *International Journal of Rock Mechanics & Mining Sciences*, 37(3), 2000, pp.509-515.
12. Weng, L., Huang, L., Taheri, A., Li, X., "Rockburst characteristics and numerical simulation based on a strain energy density index: A case study of a roadway in Linglong gold mine, China". *Tunnelling & Underground Space Technology*, 69, 2017, pp.223-232.
13. Jiang, Q., Feng, X. T., Xiang, T. B., Su, G. S., "Rockburst characteristics and numerical simulation based on a new energy index: a case study of a tunnel at 2,500 m depth". *Bulletin of Engineering Geology & the Environment*, 69(3), 2010, pp.381-388.
14. Qiu, S., Feng, X., Jiang, Q., Zhang, C., "A novel numerical index for estimating strainburst vulnerability in deep tunnels". *Chinese Journal of Rock Mechanics & Engineering*, 33(10), 2014, pp.2007-2017.
15. Su, G. S., Feng, X. T., Jiang, Q., Chen, G. Q., "Study on new index of local energy release rate for stability analysis and optimal design of underground rockmass engineering with high geo-stress". *Chinese Journal of Rock Mechanics and Engineering*, 25(12), 2006, pp.2453-2460.
16. Mansurov, V. A., "Prediction of rockbursts by analysis of induced seismicity data". *International Journal of Rock Mechanics & Mining Sciences*, 38(6), 2001, pp.893-901.
17. Zhuang, D. Y., Tang, C. A., Liang, Z. Z., Ma, K., Wang, S. Y., "Effects of excavation unloading on the energy-release patterns and stability of underground water-sealed oil storage caverns". *Tunnelling & Underground Space Technology Incorporating Trenchless Technology Research*, 61, 2017, pp.122-133.
18. Wang, G. F., Gong, S. Y., Li, Z. L., Dou, L. M., Cai, W., "Evolution of Stress Concentration and Energy Release Before Rock Bursts: Two Case Studies from Xingan Coal mine, Hegang, China". *Rock Mechanics & Rock Engineering*, 49(8), 2016, pp.3393-3401.
19. Wang, L., Lu, Z. L., Gao, Q., "A numerical study of rock burst development and strain energy release". *International Journal of Mining Science and Technology*, 22(5), 2012, pp.675-680.
20. Linkov, A. M. "Rockbursts and the instability of rock masses". *International Journal of Rock Mechanics & Mining Sciences & Geomechanics Abstracts*, 33(7), 1996, pp.727-732..
21. Gong, Q. M., Yin, L. J., Wu, S. Y., Zhao, J., Ting, Y., "Rock burst and slabbing failure and its influence on TBM excavation at headrace tunnels in Jinping II hydropower station". *Engineering Geology*, 124(1), 2012, pp.98-108.
22. Zhou, J., Li, X., Mitri, H. S., "Classification of Rockburst in Underground Projects: Comparison of Ten Supervised Learning Methods". *Journal of Computing in Civil Engineering*, 30(5), 2016, pp.04016003.
23. Feng, X. T., Yu, Y., Feng, G. L., Xiao, Y. X., Chen, B. R., "Fractal behaviour of the microseismic energy associated with immediate rockbursts in deep, hard rock tunnels". *Tunnelling & Underground Space Technology Incorporating Trenchless Technology Research*, 51, 2016, pp.98-107.
24. Trinh, N., Jonsson, K., "Design considerations for an underground room in a hard rock subjected to a high horizontal stress field at Rana Gruber, Norway". *Tunnelling & Underground Space Technology Incorporating Trenchless Technology Research*, 38(3), 2013, pp.205-212.
25. Li, X. B., Weng, L., "Numerical investigation on fracturing behaviors of deep-buried opening under dynamic disturbance". *Tunnelling and Underground Space Technology*, 54, 2016, pp.61-72
26. Li, X. B., Li, C., Cao, W. Z., Tao, M., "Dynamic stress concentration and energy evolution of deep-buried tunnels under blasting loads". *International Journal of Rock Mechanics and Mining Sciences*, 104, 2018, pp.131-146